Materials Science-Poland, 30(2), 2012, pp. 121-130
http://www.materialsscience.pwr.wroc.pl/
DOI: 10.2478/s13536-012-0019-y

The correlation between coordination and bond angle distribution in network-forming liquids

N.V. HONG*, N.V. HUY, P.K. HUNG

Institute of Engineering Physics, Hanoi University of Science and Technology, No 1 Dai Co Viet Road, Hanoi, Vietnam

The structure and diffusion in SiO_2 and Al_2O_3 liquids under pressure have been studied by molecular dynamics simulation. We show that although different states of considered liquids differ significantly in the number of TO_x units and OT_y linkages (T = Si, Al; x = 4, 5, 6; y = 2, 3, 4), their partial bond angle distributions (BAD) are identical. Furthermore, the total BADs are directly related to the partial BADs and coordination distribution. This result supports a technique to determine the fraction of TO_x and OT_y from the experimental bond angle distribution. The simulation also reveals the anomalous behavior of diffusion in silica liquid caused by the change in diffusion mechanisms occurring in low- and high-density models. The diffusion in alumina liquid also results from a similar mechanism like the one for high-density sample of silica liquid.

Keywords: *simulation, bond angle distributions, silica, alumina, diffusion mechanism*

1. Introduction

Silica and alumina are of important relevance in many technology fields such as electronics, metallurgy, ceramic materials, *etc*. At ambient pressure, the most stable crystal phases of silica and alumina are α-quartz and corundum. The melting temperature is 1980 K and 2326 K for silica and alumina, respectively. At the liquid state, the structure of silica as well as alumina is believed to be composed of TO_x units connected to each other by bridging oxygen atoms. The microstructure change in those liquids under pressure is of great interest and has been intensively studied for a long time [1–5]. It was found that when applying pressure, the liquid silica undergoes a transformation from tetrahedral to octahedral network structure. Upon pressure lower than 5 GPa, the structure of liquid silica comprises mainly of SiO_4 tetrahedra [6–12]. As shown by X-ray Synchrotron Radiation, Neutron Diffraction and NMR experiments in [12–14], at ambient pressure, the liquid alumina also consists of AlO_5 and AlO_6 species besides AlO_4. The average coordination number of aluminum is 4.5. At a pressure higher than 20 GPa, both liquid silica and alumina consist mainly of TO_6 species.

The microstructure can be described by bond angle distribution measured by X-ray diffraction, Neutron Diffraction and NMR method. The experimental results in [15, 16] show that the mean Si–O–Si bond angle for amorphous silica varies from 142° to 160° and full width half maximum (FWHM) of BAD varies in a wide range from 10° to 46°. High pressure X-ray diffraction experiment in [1] revealed that O–Si–O BAD decreases as the pressure increases; at 42 GPa, the mean O–Si–O bond angle is 96°. This is an intermediate value between 90° (for tetrahedral network) and 109.5° (for octahedral network). Because molten silica evaporates very quickly at temperatures above 2140 K, there are only few experimental works for liquid silica [17]. A recent investigation shows that the bigger size of the SiO_4 tetrahedrons in melted silica induces the decrease of the mean Si–O–Si bond angle in comparison with amorphous silica [18]. In case of amorphous alumina, X-ray and Neutron Diffraction experiments show that the structure is built up by AlO_4 and that the Al–O–Al bond angle, between two corner sharing tetrahedrons, is about 125° [8].

Because of difficulty in performing the experimental studies at high temperature, at present, simulation methods are still useful tools for studying the structure of liquid silica and alumina, especially at

*E-mail: hongnv-iep@mail.hut.edu.vn

high temperatures and pressures. Classical molecular dynamics (MD) simulations can get insight into the structure and dynamics properties of liquid silica and alumina under high pressure [19–22]. The simulation results in recent works concerning silica and alumina reveal that a gradual transition from tetrahedral to octahedral coordination induces the variation of total O–T–O and T–O–T BAD. It means that there is a correlation between the total O–T–O, T–O–T BADs and coordination distribution. Basing on this correlation, one can determine the fraction of TO_x and OT_y units from the experimental BADs. For a network-forming liquid, the dynamics properties and diffusion depend strongly on TO_x fraction in the model [20], thus this correlation also allows the estimation of diffusion. However, as far as we know, no other works have been done to clarify the correlation between the total O–T–O, T–O–T BADs and coordination distribution. Specially, the anomalous diffusion in silica is still in debate.

In this work, the structural characteristics of liquid silica and alumina are investigated in detail in order to find the correlation between the total BADs and coordination distribution. The diffusion mechanism in these materials, especially the anomalous diffusion in silica is also analyzed and discussed here.

2. Computational procedure

Molecular dynamics simulations are carried out on silica and alumina models consisting of 1998 and 2000 atoms respectively. The simulation has been performed in a cubic cell where the periodic boundary conditions were applied. The BKS and Born Mayer potentials are used to construct SiO_2 and Al_2O_3 models, respectively. More detail about these potentials can be found elsewhere [19, 23, 24]. The initial configuration is generated by placing all atoms randomly in a simulation box and heating it up to 5000 K to remove possible memory effects. Afterward, the sample is cooled down to 4500, 4000, 3500 and finally to 3000 K with a rate of 0.25 K/ps. The equation of motion is integrated using the Verlet algorithm with a time step of 0.46 fs. At temperatures of 4500, 4000 and 3500 K, a relaxation with 2×10^4 time steps is accomplished and then a 10^6 time step relaxation is performed to produce a model at 3000 K, upon ambient pressure. Hereafter, the obtained model is called S0/A0 corresponding to silica/alumina. Next, we produce six different models of SiO_2 and Al_2O_3 by subjecting the model S0 or A0 to different pressures. More details about this calculation can be found in [22]. The structural data of considered models are determined by averaging over 2000 configurations during the last 10^4 time steps. To calculate the coordination number and bond angle, we use the cut-off distance R_{Si-O} = 2.38 Å and R_{Al-O} = 2.56 Å. Here, R_{Si-O} and R_{Al-O} are chosen as the first minimum after the peak of pair distribution functions (PDF) for silica (at the density of 3.44 g·cm^{-3}) and alumina (at the density of 3.20 g·cm^{-3}) respectively.

3. Results and discussion

The structural characteristics of liquid silica and alumina models are presented in Table 1 and 2, respectively. For liquid silica, the results show that at low density (2.61 g·cm^{-3}), about 94 % Si atoms have tetrahedral coordination with a mean coordination number of Z_{Si-O} = 4.05, 97 % O atoms have twofold coordination with a mean coordination number of Z_{O-Si} = 2.03. This reveals that at low density, the structure of liquid silica is built up by SiO_4 tetrahedrons and forms a simple continuous random network of corner-sharing tetrahedrons. For liquid alumina, the results show that at low density (2.71 g·cm^{-3}), the Al–O coordination number distribution is characterized by the frequencies of 4 (66 %), 5 (29 %) and 6 (3 %) with a mean coordination number of Z_{Al-O} = 4.30. The coordination number distribution O–Al is characterized by the frequencies 2 (22 %), 3 (70 %) and 4 (8 %) with a mean coordination number of Z_{O-Al} = 2. 86. This means that at low density, the structure of liquid alumina is built up by AlO_4 and AlO_5 units and forms a continuous random network of these units. The simulation results for liquid silica and alumina show a good agreement with experimental data as well as the simulations of other works in bond length, coordination number and bond angle [1, 8, 12, 13, 15, 16, 19, 21, 29]. Now, we will focus on investigating BAD and establishing the correla-

Table 1. Structural characteristics of liquid silica. r_{xy} – position of the first peak of PDF $g_{xy}(r)$; Z_{xy} – the mean coordination number; Si_x, O_y – the fraction of structural SiO_x units and OSi_y linkages.

Models	M1	M2	M3	M4	M5	M6	References		
ρ, g·cm^{-3}	2.61	3.09	3.44	3.69	3.87	4.04	[a]2.20	[b]2.67	
Z_{Si-O}	4.05	4.37	4.75	5.07	5.39	5.44		[d]4.0	[c]3.88±0.20
Z_{O-Si}	2.03	2.18	2.38	2.53	2.70	2.72		[d]2.0	
r_{Si-Si}, Å	3.08	3.08	3.08	3.08	3.08	3.08	[a]3.065	[b]3.00	
r_{Si-O}, Å	1.60	1.60	1.60	1.62	1.62	1.64	[a]1.626	[b]1.60	[c]1.626
r_{O-O}, Å	2.60	2.58	2.50	2.50	2.46	2.42		[b]2.60	
$<\theta_{O-Si-O}>$	107°	105°	103°	103°	102°	102°	[a]109.43°	[b]09°	[c]107°±2°
$<\theta_{Si-O-Si}>$	143°	131°	123°	119°	117°	116°	[a]143.38°	[b]141°	[c]128÷136°
Si_4	0.94	0.66	0.38	0.21	0.10	0.07			
Si_5	0.05	0.31	0.49	0.51	0.43	0.44			
Si_6	0.00	0.03	0.13	0.27	0.45	0.47			
O_2	0.97	0.81	0.63	0.48	0.35	0.32			
O_3	0.03	0.19	0.36	0.50	0.63	0.66			
A	0.16	0.13	0.11	0.10	0.08	0.07			
B	0.95	0.74	0.55	0.46	0.41	0.39			

[a,b,c,d]Experimental data given in [25], [26], [18] and [28] respectively

Table 2. Structural characteristics of liquid alumina. r_{xy} – position of the first peak of PDF $g_{xy}(r)$; Z_{xy} – the mean coordination number; Al_x, O_y – the fraction of structural AlO_x units and OAl_y linkages.

Models	M1	M2	M3	M4	M5	M6	References		
ρ, g·cm^{-3}	2.71	2.98	3.20	3.40	3.56	3.68	[a]2.81	[b]2.81	[c] 3.175
Z_{Al-O}	4.30	4.50	4.73	4.93	5.14	5.29	[a]4.20	[b]4.20	[c]4.10
Z_{O-Al}	2.86	3.50	3.15	3.29	3.43	3.53	–	–	[c]2.72
r_{Al-Al}, Å	3.14	3.12	3.08	3.06	3.04	3.04	–	[b]3.25	[c]3.15
r_{Al-O}, Å	1.68	1.70	1.70	1.72	1.72	1.72	[a]1.76	[b]1.78	[c]1.71–1.79
r_{O-O}, Å	2.78	2.74	2.72	2.68	2.64	2.62	–	[b]2.84	[c]2.75
$<\theta_{O-Al-O}>$	105°	103°	103°	103°	102°	101°	–	–	[c]103°
$<\theta_{Al-O-Al}>$	116°	114°	111°	110°	109°	108°	–	–	[c]115°
Al_4	0.66	0.53	0.38	0.27	0.19	0.12			
Al_5	0.29	0.39	0.50	0.54	0.50	0.49			
Al_6	0.03	0.06	0.12	0.19	0.30	0.37			
O_2	0.22	0.14	0.07	0.04	0.02	0.01			
O_3	0.70	0.72	0.71	0.64	0.55	0.48			
O_4	0.08	0.14	0.21	0.31	0.41	0.48			
A	0.14	0.12	0.11	0.10	0.09	0.09			
B	0.36	0.32	0.29	0.26	0.24	0.22			

[a]Experimental data at ambient pressure given in [12]
[b]Experimental data at ambient pressure given in [13]
[c]Simulation data at ambient pressure given in [10]

tion between coordination number distribution and BADs. We only consider O–T–O and T–O–T bond angle. The first describes the topology structure of TO_x units and the second describes the connectivity between the TO_x units. From Tables 1 and 2, it can be seen that there is a gradual transition from the tetrahedral coordination to the fivefold and sixfold coordinations with increasing the density. The

fraction of TO_4 units decreases monotonously from 94 % (for silica at density 2.61 g·$mathrmcm^{-3}$) and 66 % (for alumina at density 2.71 g·cm^{-3}) to 7 % (for silica at density of 4.04 g·cm^{-3}) and 12 % (for alumina at density of 3.68 g·cm^{-3}). Conversely, the fraction of TO_6 increases monotonously, whereas the fraction of TO_5 increases gradually up to the maximum value (51 % for silica, 54 % for alumina) and then decreases gradually.

The connection between TO_x units through an O bridge forms an OT_y linkage. For liquid silica, most of the linkages are made of OSi_2 and OSi_3; the fraction of OSi_4 linkages is very small.

To establish the correlation between the coordination number distribution and total O–T–O BAD, let n_{Tx} be the number of TO_x units; here $x = 4, 5$ and 6. The total number of O–T–O angles in TO_4, TO_5 and TO_6 is $6n_{T4}$, $10n_{T5}$ and $15n_{T6}$, respectively. We ascribe $m_{Tx}(\theta)$ to the number of angles in an interval of $\theta \pm d\theta$ in TO_x units. The probability that a given angle lies in the interval $\theta \pm d\theta$ in a sample, is given by

$$\begin{aligned} g_T(\theta) &= \frac{m_{T4}(\theta)+m_{T5}(\theta)+m_{T6}(\theta)}{6n_{T4}+10n_{T5}+15n_{T6}} \\ &= 6Ag_{T4}(\theta)T_4+10Ag_{T5}(\theta)T_5 \\ &\quad +15Ag_{T5}(\theta)T_5 \end{aligned} \tag{1}$$

where $A = (n_{T4}+n_{T5}+n_{T6})/(6n_{T4}+10n_{T5}+15n_{T6})$; $g_{T4}(\theta) = m_{T4}(\theta)/6n_{T4}$; $g_{T5}(\theta) = m_{T5}(\theta)/10n_{T5}$; $g_{T6}(\theta) = m_{T6}(\theta)/15n_{T6}$. The function $g_{Tx}(\theta)$, actually represents the probability that the given O–T–O angle in TO_x units lies in the interval of $\theta \pm d\theta$. Therefore, the function $g_T(\theta)$ describing the total O–T–O BAD can be expressed via the fraction of T_x and the functions $g_{Tx}(\theta)$ which represent the partial BAD for the TO_x units. Here, the notation T_x (T = Si or Al; x = 4, 5, 6) is the fraction of TO_x in the sample. The values of T_x (Si_x for liquid silica, Al_x for liquid alumina) are given in Table 1 and Table 2. Previous works [15] showed that, upon compression, the TO_x fractions vary strongly, but the topology of the TO_x units is unchanged, *e.g.* the liquids with different density consist of identical TO_x units. It means that there are the common functions $g_{Tx}(\theta)$ for all considered models. These functions are presented in Figs. 1 and 2. For TO_4, the function $g_{T4}(\theta)$ has a form of Gauss function with a pronounced peak at 105°; in the case of TO_5, the function $g_{T5}(\theta)$ has a peak and a shoulder: a main peak is located at 90° (for silica), 85° (for alumina), the shoulder is at 165° for both silica and alumina; for TO_6, the function $g_{T6}(\theta)$ has a pronounced peak at 85° (for silica), 80° (for alumina) and a small peak at 160°.

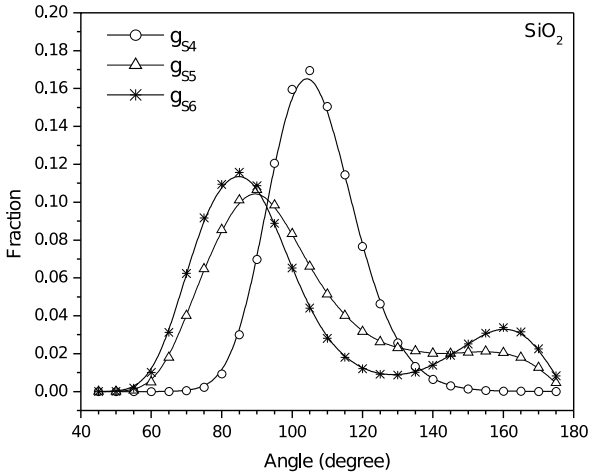

Fig. 1. The partial O–Si–O angle distribution functions $g_{Sx}(\theta)$ for basic units SiO_x.

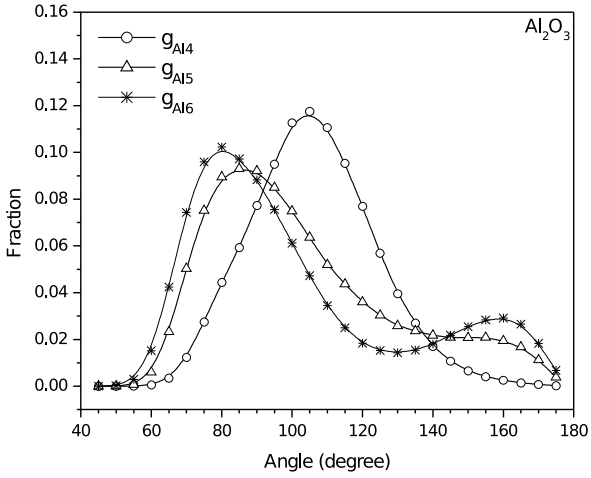

Fig. 2. The partial O–Al–O angle distribution functions $g_{Alx}(\theta)$ for basic units AlO_x.

Figs. 3 and 4 show the total O–T–O BADs for silica and alumina models together with the result calculated by Equation (1) at different densities. It can be seen that the total O–T–O BAD changes significantly with density. Its main peak slightly

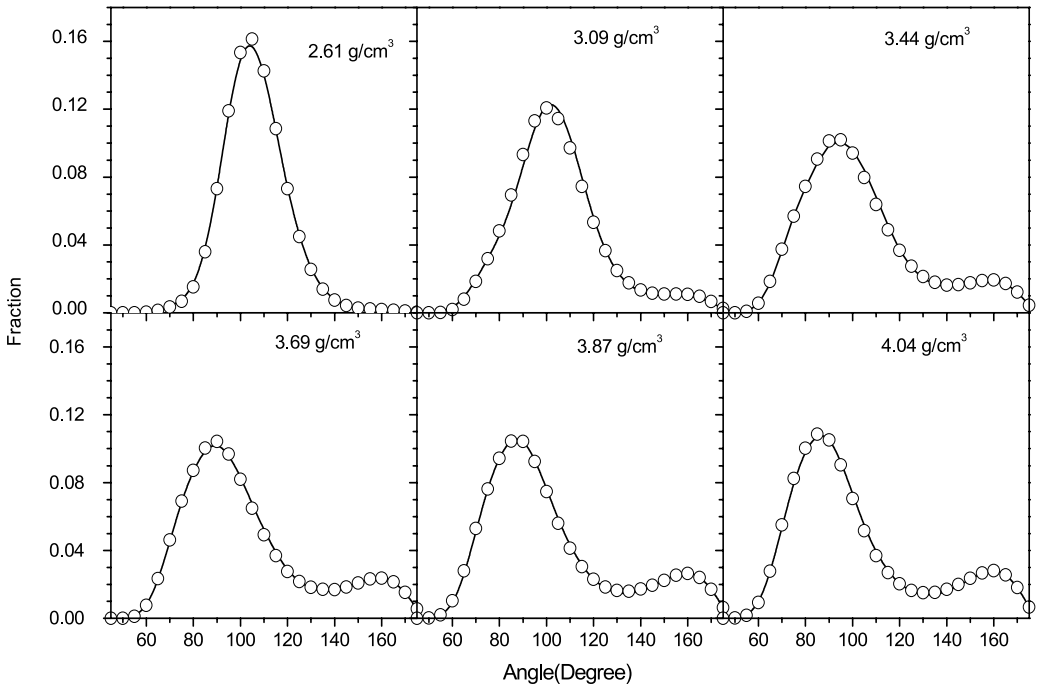

Fig. 3. The total O–Si–O bond angle distribution; the symbols present simulation data; the lines present data calculated by Equation (1).

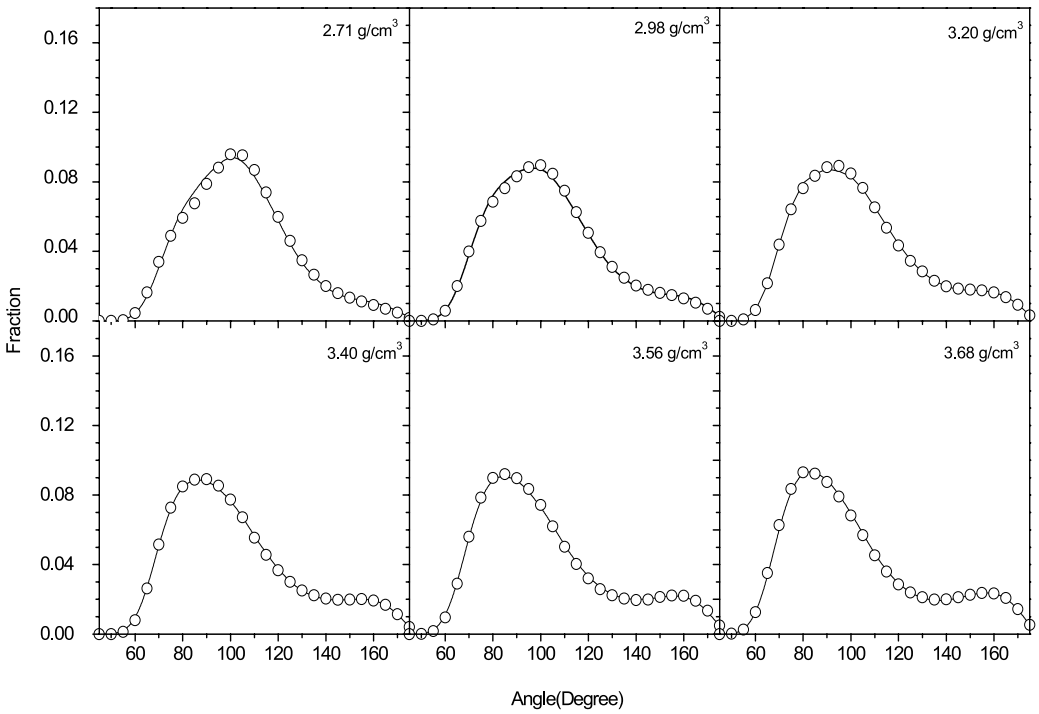

Fig. 4. The total O–Al–O bond angle distribution; the symbols present simulation data; the lines present data calculated by Equation (1).

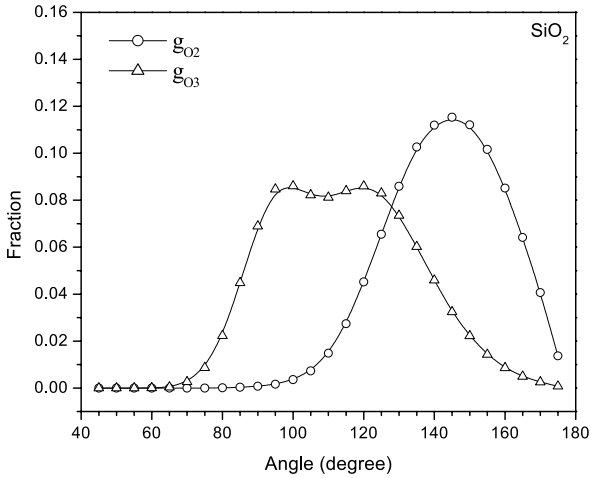

Fig. 5. The partial Si–O–Si bond angle distribution functions $g_{Oy}(\theta)$ for OSi_y linkages.

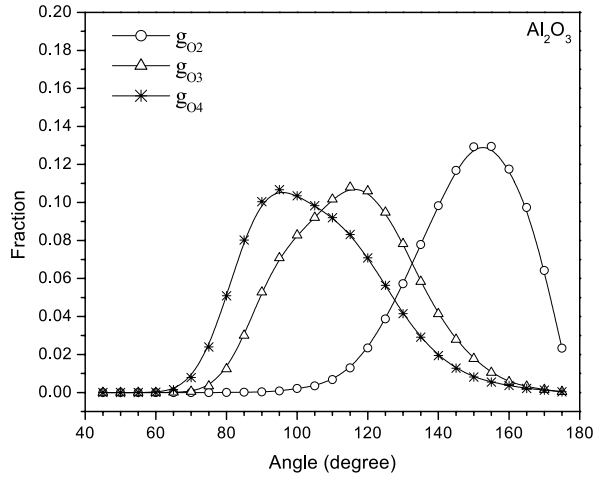

Fig. 6. The partial Al–O–Al bond angle distribution functions $g_{Oy}(\theta)$ for OAl_y linkages.

shifts to lower angles and the height of the main peak decreases with the density. Furthermore, it is clear that the calculation results reproduce very well the simulation data indicating a way to extract the fraction of TO_x units on the base of known functions $g_{Tx}(\theta)$. In similar way, the total T–O–T BAD can be given as

$$\begin{aligned} g_O(\theta) &= \frac{m_{O2}(\theta)+m_{O3}(\theta)+m_{O4}}{n_{O2}+3n_{O3}+6n_{O4}} \\ &= Bg_{O2}(\theta)O_2+3Bg_{O3}(\theta)O_3 \\ &\quad +6Bg_{O4}(\theta)O_4 \end{aligned} \tag{2}$$

where $g_{O2}(\theta)=m_{O2}(\theta)/n_{O2}$; $g_{O3}(\theta)=m_{O3}(\theta)/n_{O3}$; $g_{O4}(\theta)=m_{O4}(\theta)/n_{O4}$; $B=(n_{O2}+n_{O3}+n_{O4})/(n_{O2}+3n_{O3}+6n_{O4})$. Similar to $g_{Tx}(\theta)$, the function $g_{Oy}(\theta)$ represents the probability that the given T–O–T angle in OT_y lies in the interval of $\theta \pm d\theta$.

The partial bond angle distributions for OT_y are shown in Figs. 5 and 6. For OT_2 linkages, $g_{O2}(\theta)$ has a main peak at 145° (for silica), 153° (for alumina); in the case of OT_3 for silica, the function $g_{O3}(\theta)$ has two peaks at 100° and 120° but for alumina it only has one peak at 115°. In contrast to liquid silica, the fraction of OAl_4 linkages in liquid alumina is rather high (48 % at density $\rho = 3.68$ g·cm^{-3}) and the function $g_{O4}(\theta)$ has a peak at 95°.

The total T–O–T BADs are shown in Figs. 7 and 8. It can be seen that with increasing density, the total T–O–T bond angle shifts to lower angles. For liquid silica, the total Si–O–Si BAD shifts to lower angles then splits into two peaks. The main peak that is located at 143°, splits into two sub-peaks at about 95° and 130° as the density is higher than 3.44 g·cm^{-3}. For alumina, at density of 2.71 g·cm^{-3}, $g_O(\theta)$ has a peak at about 118°, this peak shifts to 100° at density of 3.68 g·cm^{-3}. The results also reveal that there is a good agreement between the simulation results and the data calculated by Equation (2).

Fig. 9 shows the pressure dependence of diffusion coefficient in liquid silica and alumina. It can be seen that the diffusion coefficient of Si atoms in liquid silica is similar to O atoms. It also shows anomalous behavior. The diffusion coefficient approaches its maximum at a pressure of about 12 GPa, which is similar to the results in references [30–32]. In the case of liquid alumina, the diffusion coefficient of Al as well as O atoms decreases with pressure. The pressure dependence of the diffusion coefficient of atoms in alumina is similar to the one in silica at a pressure higher than 12 GPa. To clarify the diffusion mechanism that causes the anomalous diffusion in liquid silica we have investigated the displacement and the process of neighbor change for the atoms in the models.

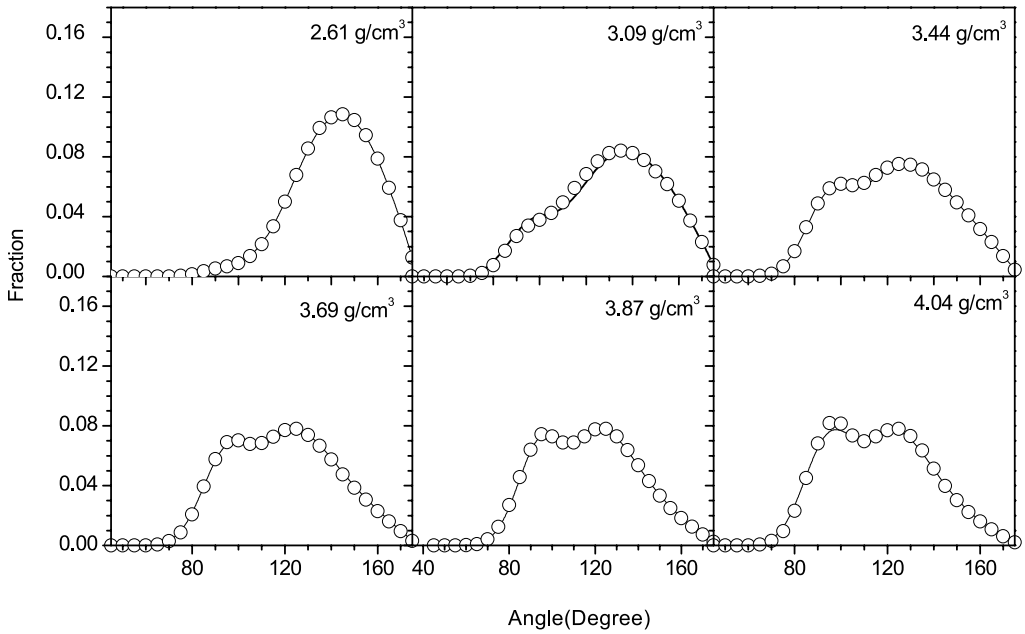

Fig. 7. The total Si–O–Si bond angle distribution; the symbols present simulation data; the lines present data calculated by Equation (2).

Table 3. The frequency of changing the neighbor of Si and O at the 5000, 20000 and 40000 run steps.

		5000 steps		20000 steps		40000 steps	
P(GPa)	ρ, g·cm^{-3}	Si	O	Si	O	Si	O
0	2.61	659	1165	707	1366	701	1377
5	3.09	214	410	221	438	223	442
10	3.44	144	280	145	288	146	289
15	3.69	126	245	128	253	129	257
20	3.87	121	235	121	239	121	240
25	4.04	119	231	118	234	106	233

Table 3 shows the frequency of changing the neighbor of Si and O after the 5000, 20000 and 40000 time steps. Although the fraction of SiO_x in the model at a given pressure is definite, the neighbors of atoms are always changed and this change causes the movement of atoms. It can be seen that the frequency of changing the neighbor of an atom does not depend on the run time but on the pressure. At ambient pressure (run time is over 20000 steps), the frequency of changing the neighbor of Si and O is about 700 and 1370 time steps respectively. At 25 GPa, the frequency of changing the neighbor of Si and O is about 110 and 230 time steps, respectively. The more frequently atoms change their neighbors, the higher mobility they get. This explains the increase in diffusion coefficient as the pressure or density increases. The data in Table 3 also show that the frequency of changing the neighbor increases strongly as the pressure increases from 0 to 10 GPa. This is due to the considerable increase of the fraction of SiO_5 units and OSi_3 linkages as the pressure increases. The SiO_5 unit and OSi_3 linkage is unstable so that Si and O atoms in SiO_5 and OSi_3 can easily change their neighbor. In the range from 10 to 25 GPa, the frequency of changing the neighbor varies only slightly because the fractions of SiO_5 and OSi_3 almost do not change (see Table 1). It means that the frequency of changing the

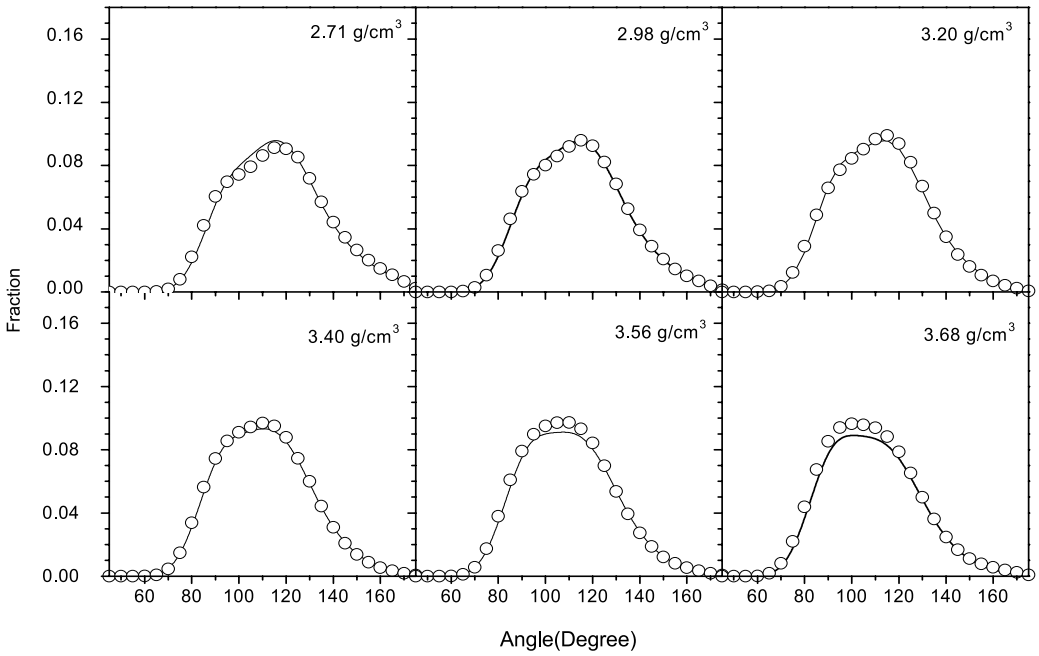

Fig. 8. The total Al–O–Al bond angle distribution; the symbols present simulation data; the lines present data calculated by Equation (2).

Table 4. Effect of pressure on the change of neighbor of atoms in the model after 40000 run steps.

n	0 GPa		5 GPa		10 GPa		15 GPa		20 GPa		25 GPa	
	Si	O	Si	O	Si	O	Si	O	Si	O	Si	O
0	464	1107	29	287	0	93	10	122	4	94	16	160
1	166	205	139	617	29	420	53	488	32	459	68	547
2	30	20	236	381	102	613	129	549	116	558	162	476
3	5	0	160	46	214	194	203	165	219	214	198	144
4	1	0	82	1	219	12	190	8	174	7	158	5
5			18	0	87	0	53	0	99	0	51	0
6			2	0	15	0	28	0	21	0	13	0
7									1	0		

neighbor depends strongly on the fraction of SiO_5 and OSi_3 in the model.

Table 4 displays the effect of pressure on the change of neighbor of atoms after 40000 run steps. At ambient pressure (0 GPa), most of atoms do not change their neighbors (464 Si atoms and 1107 atoms do not change any neighbor); 166 Si atoms and 205 O atoms change one neighbor; 30 Si atoms and 20 O atoms change two neighbors; 5 Si atoms change three neighbors; only one Si atom change all four neighbors. At 25 GPa, most atoms change their neighbors after 40000 run steps; only 16 Si atoms and 160 O atoms do not change any neighbor. This demonstrates again that the mobility of atoms increases with increasing pressure.

The results in Table 5 show that the average displacement of one atom after one time changing neighbor decreases as the pressure increases. After 5000 run steps, this average displacement decreases from 0.196 Å at 0 GPa to 0.032 Å at 25 GPa. After 40000 run steps, the average displacement of one atom after one time changing neighbor decreases from 0.111 Å at 0 GPa down to 0.024 Å. Table 5 also shows that as the number of run steps increases

Table 5. The average displacement of atom after one time changing the neighbor at 5000, 20000 and 40000 time steps.

Time steps	Average displacement/one time changing neighbor					
	0 GPa	5 GPa	10 GPa	15 GPa	20 GPa	25 GPa
5000	0.196	0.053	0.039	0.036	0.033	0.032
20000	0.147	0.043	0.031	0.028	0.026	0.026
40000	0.111	0.039	0.032	0.028	0.025	0.024

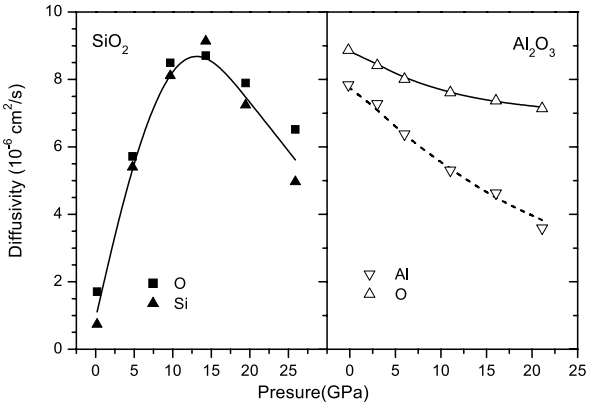

Fig. 9. The diffusivity as a function of pressure.

then the average displacement of one atom after one time changing neighbor decreases. At ambient pressure, it is 0.196 Å after 5000 run steps, 0.147 Å after 20000 run steps, 0.111 Å after 40000 run steps. This can be explained as follows: the time evolution of the mean square displacement $r^2(t)$ consists of three time stages (see Fig. 10). The first stage is a ballistic motion (short time, about 500 time steps). The second stage is the caging stage in that the particles are temporarily trapped in the cages formed by their neighbors. The third stage is a diffusive motion (long time). From above analysis, it can be seen that the diffusion mechanism in silica liquid is caused by the change of neighbor atoms. There are two mechanisms causing the anomalous behavior: 1) the increase in frequency of changing neighbor as the pressure increases, which results in increasing the diffusion coefficient; 2) the decrease in the average displacement of an atom after one time changing neighbor as the pressure increases, which causes the decrease in the diffusion coefficient. The combination of the two mechanisms results in the maximum of diffusion coefficient in the range of considered pressures (from 0 to 25 GPa), see Fig. 9.

4. Conclusions

We have constructed six models of liquid silica with different density in the range from 2.61 to 4.04 g·cm^{-3} and six models of liquid alumina with density in the range from 2.71 to 3.68 g·cm^{-3}. The structural characteristics of the constructed models are in good agreement with the experimental results as well as with the simulation results of other works. The results of our studies led us to the conclusion that liquid silica and alumina undergo significant variation in the network structure, leading to the change in the number of TO_x polyhedrons and OT_y linkages. The topology structure of these polyhedrons and linkages is identical for all constructed models. Consequently, all the models have the same partial bond angle distributions $g_{Tx}(\theta)$ and $g_{Oy}(\theta)$. This result enables us to establish a simple relationship between the bond angle distribution and the fractions of TO_x polyhedrons and OT_y linkages. The simulation results show a good agreement with the data calculated by the obtained expression for both total T–O–T and O–T–O BADs. Diffusion in liquid silica shows anomalous behavior. Diffusion mechanism is caused by the change of neighbors. Two competing mechanisms that result in the anomalous diffusion in liquid silica are the increase of frequency of neighbor change and the decrease of average displacement after one time changing neighbor as the pressure increases. The dependence of diffusion coefficient on pressure (density) has a maximum at a pressure of about 12 GPa.

Acknowledgements

This research is funded by Vietnam National Foundation for Science and Technology Development (NAFOSTED) under grant number 103.99-2011.22.

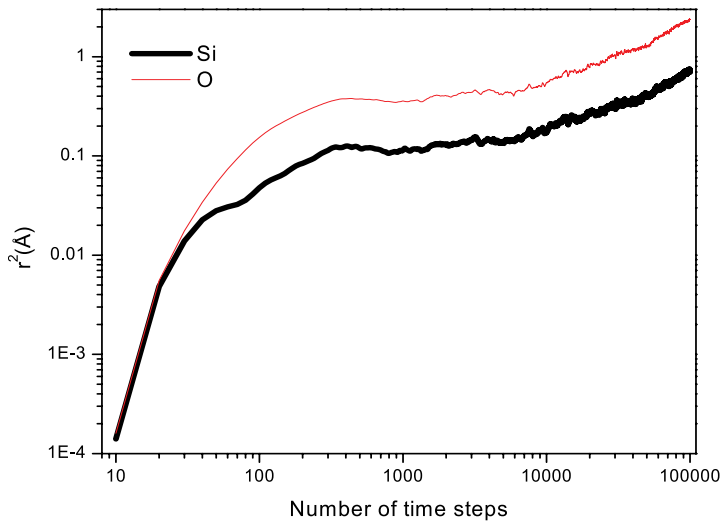

Fig. 10. The dependence of mean square displacement on the number of run steps knowledgement.

References

[1] MEADE C., HEMLEY R.J., MAO H.K., *Phys. Rev. Lett.*, 69 (1992), 1387.

[2] LACKS D.J., *Phys. Rev. lett.*, 84 (2000), 4629.

[3] STIXRUDE L., BUKOWINSKI M.S.T., *Phys. Rev B*, 44 (1991), 2523.

[4] RUSTAD J.R., YUEN D.A., SPERA F.J., *Phys. Rev A*, 42 (1990), 2081.

[5] YAMADA A., WANG Y, INOUE T., YANG W., PARK CH, YU T., SHEN G., *Rev. Sci. Instrum.*, 82 (2011), 015103.

[6] PETTIFER R.F., DUPREE R., FARNAN I., STERNBERG U., *J. Non-cryst. Solids*, 106 (1988), 408.

[7] ARTEM R.O., MICHAEL J.G., PRICE G.D., *Phys. Rev B*, 71 (2005), 064104.

[8] LAMPARTER P., KNIEP R., *Physica B*, 234–236 (1997), 405–406.

[9] ANSELL S. et al., *Phys. Rev. Lett.*, 78 (1997), 464.

[10] GUTIERREZ G., BELONOSHKO A.B., AHUJA R., JOHANSSON B., *Phys. Rev. E*, 61 (2000), 2723.

[11] GUTIERREZ G., JOHANSSON B., *Phys. Rev. B*, 65 (2002), 104202.

[12] LANDRON C, SOPER A.K., JENKINS T.E., GREAVES G.N., KENNET L., COUTURES J.P., *J. Non-cryst. Solids*, 293–295 (2001), 453.

[13] LANDRON C., HENNET L., JENKINS T.E., GREAVES G.N., COUTURES J.P., SOPER A.K., *Phys. Rev. Lett.*, 86 (2001), 4839.

[14] HUNG P.K., NHAN N.T., VINH L.T., *Modelling Simul. Mater. Sci. Eng.*, 17 (2009), 025003.

[15] WIM J.M., WERNER E.H., RENE V., *Chemical Geology*, 256 (2008), 269.

[16] KUBICKI J.D., LASAGA A.C., *American Mineralogist*, 73 (1988), 941.

[17] SCHNURRE S.M., GROBNER J., SCHMID F.R., *J. Non-cryst. Solids*, 336 (2004), 1.

[18] MEI Q., BENMORE C.J., AND WEBER J.K.R., *Phys. Rev. Lett.*, 98 (2007), 057802.

[19] HORBACH J., *J. Phys.: Condens. Matter.*, 20 (2008), 244118.

[20] HUNG P.K., HONG N.V., *Eur. Phys. J. B*, 71 (2009), 105.

[21] HOANG V.V., KUN O.S., *Phys. Rev B*, 72 (2005), 054209.

[22] HUNG P.K., VINH L.T., NHAN N.T., HONG N.V., MUNG T.V., *J. Non-cryst. Sol.*, 354 (2008), 3093.

[23] YUAN X., CORMACK A.N., *J. Non-Cryst. Sol.*, 283 (2001), 69.

[24] HUNG P.K., HONG N.V., VINH L.T., *J. Phys.: Condens. Matter.*, 19 (2007), 466103.

[25] LEVELUT C., CABARET C., BENOIT M., JUND P., FLANK A.M., *J. Non-Cryst. Sol.*, 293–295 (2001), 100.

[26] SUSMAN S., VOLIN K.J., PRICE D.L., GRIMSDITCH M., RINO J.P., KALIA R.K., VASHISHTA P., GWANMESIA G., WANG Y., LIEBERMANN R.C., *Phys. Rev. B*, 43 (1991), 1194.

[27] MEI Q., BENMORE C.J., SEN S., SHARMA R., YARGER J.L., *Phys. Rev. B*, 78, 144204 (2008).

[28] MOZZI R.L., WARREN B.E., *J. Appl. Cryst.*, 2 (1969), 164.

[29] TED M.C., PHILIP J.G., *Phys. Rev. B*, 70 (2004), 064202.

[30] SHELL M.S., PABLO G.D., ATHANASSIOS Z.P., *Phys. Rev E*, 66 (2002), 011202.

[31] BIJAYA B.K., BHATTARAI D., STIXRUDE L., *Phys. Rev. B*, 76 (2007), 104205.

[32] TSUNEYUKI S., MATSUI Y., *Phys. Rev. Lett.*, 74 (1995), 3197.

Received 23.02.2012
Accepted 03.06.2012